

ENTHALPIC STUDY OF STRUCTURAL RELAXATION AND CRYSTALLIZATION IN SOME METALLIC GLASSES

M. Baricco, L. Battezzati and G. Riontino

ISTITUTO DI CHIMICA GENERALE ED INORGANICA
FACOLTÀ DI FARMACIA UNIVERSITÀ DI TORINO
VIA P. GIURIA, 9 — 10125 TORINO, ITALY

Structural relaxation and crystallization have been studied in the metallic glasses $\text{Fe}_{39}\text{Ni}_{36}\text{Cr}_5\text{P}_{14}\text{B}_6$, $\text{Fe}_{81}\text{B}_{19}$, $\text{Fe}_{76}\text{Co}_4\text{B}_{20}$ and $\text{Fe}_{75}\text{V}_4\text{B}_{21}$ by DSC.

Different coefficients of calibration of the DSC cell were determined for the two phenomena.

The enthalpy of relaxation increases with increasing quenching rate for $\text{Fe}_{39}\text{Ni}_{36}\text{Cr}_5\text{P}_{14}\text{B}_6$ and with increasing number of alloy components for Fe-B-based glasses. In the latter systems, relaxation is never completed before the start of crystallization.

The enthalpy of crystallization does not depend on the quenching rate for $\text{Fe}_{39}\text{Ni}_{36}\text{Cr}_5\text{P}_{14}\text{B}_6$, and does not change during annealing within the relaxation field before crystallization.

Metallic glasses are produced by the very rapid quenching of molten alloys to suppress crystal solidification and to attain an amorphous metastable state. It has been clearly established in recent years that many transformations occur when an amorphous alloy is heated, and that all of them can be followed by DSC.

Within the amorphous state, structural relaxation phenomena occur. These cannot be sharply demonstrated by means of direct structural techniques, but produce strong effects on many physical properties of the material, such as the Curie temperature [1], magnetization and coercivity [2] and resistivity [3]. There are both exothermic and endothermic effects in DSC, which are commonly referred to as topological relaxation and chemical short-range ordering, respectively [4]. The former phenomenon, which will be considered in this paper, consists mainly in the annealing-out of the free volume frozen in during quenching. In fact, the amount of heat released depends strongly on the quenching rate achieved during the preparation of the samples [5]. The latter effect can be detected only after suitable thermal treatment, and is tentatively assigned to a short-range clustering of atoms, leading to more favourable chemical interactions [5, 6]. Crystallization gives sharp exothermal peaks, in some cases preceded by a step in the DSC trace, indicating the glass transition temperature, T_g .

In this paper we report first on the calibration problems that are encountered in enthalpic studies by means of DSC. Subsequently, we give some examples of enthalpic analysis in significant cases of structural relaxation and crystallization. It is commonly believed that a glassy phase transforms to undercooled liquid at the glass transition temperature. Thus, all relaxation phenomena within the amorphous state should be fully completed at T_g , and it is to be expected that crystallization following the glass transition should not be affected by the quenching rate employed in the preparation process. On the other hand, some amorphous alloys crystallize without showing a manifest T_g . In fact, in these cases crystallization is kinetically favoured with respect to glass transition, and the alloy decomposes into crystalline phases before reaching the undercooled liquid state. When crystallization starts, relaxation phenomena are still occurring and some overlapping of the two processes can be envisaged.

Experimental

Two series of alloys were rapidly quenched from the liquid state, in ribbon form, by ejecting a stream of molten alloy onto a rotating copper wheel (melt spinning technique). A first set of metallic glasses of nominal composition $\text{Fe}_{39}\text{Ni}_{36}\text{Cr}_5\text{P}_{14}\text{B}_6$ were prepared at different quenching rates by changing the speed of the wheel, which was operating at peripheral velocities of 28, 37 or 42 m/s. All other process parameters were kept constant. A second set of specimens, with compositions $\text{Fe}_{81}\text{B}_{19}$, $\text{Fe}_{76}\text{Co}_4\text{B}_{20}$ and $\text{Fe}_{75}\text{V}_4\text{B}_{21}$, were prepared at the same quenching rate by the same technique.

The amorphous state of the alloys was controlled on both sides of the ribbons by X-ray diffractometry.

Calorimetric measurements were performed on samples from 1 to 10 mg in weight by means of a DuPont 1090 thermal analyzer equipped with a 910 DSC cell working at a constant heating rate of 0.5 deg/s under a flow of purified argon.

A fundamental problem of enthalpic measurements is the determination of the DSC cell constant. We have measured the calibration coefficient, K , by recording both the specific heats of sapphire and copper 56 mg and 10, 70 and 100 mg, respectively and the heats of fusion of some pure metals (1 to 10 mg of In, Bi, Pb, Sn and Zn). The results are shown in Fig. 1 as a function of temperature. Within the accuracy of the experimental data, the calibration coefficient is constant with respect to temperature, due to the internal calibration of the instrument, but two other points can be observed from Fig. 1. First, there is a large scatter in the K values determined from the melting of pure metals and, in particular, no coincidence is

found by using enthalpy values taken from different sources. A critical evaluation of the current data therefore seems necessary, in order to improve the applicability of DSC to quantitative determinations, as also suggested by Eysel and Breuer [10], who obtained similar results with different equipment. Second, different values of the calibration coefficient are obtained, depending on the calibration method used. Lower K values, i.e. higher DSC sensitivities, are found with the specific heat

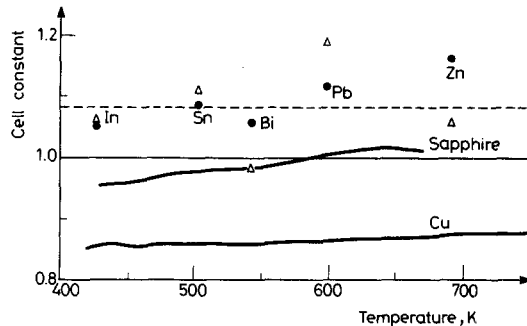


Fig. 1 Coefficient of calibration, K , vs. temperature, computed from heat of fusion and specific heat measurements. Source of data: heat of fusion, circles (7), triangles (8); specific heat, sapphire (9), Cu (7)

measurement than with the enthalpic method. Moreover, two different K levels are obtained by recording the specific heats of sapphire and copper, probably because of the difference in thermal conductivity of the two materials. This was confirmed by measuring the specific heats of copper and silver with sapphire as reference, according to the procedure described by Mraw and Naas [11]. A systematic deviation of 7–9% from selected values was observed. This is reduced to 1.5–3.5% when the specific heat of silver is measured with copper as reference. Owing to these difficulties, we decided to use two K values, for relaxation and crystallization, respectively, obtained from the most similar heat effects in the measured property. We chose $K = 1.08 \pm 0.03$ from heats of fusion for crystallization, and $K = 0.99 \pm 0.03$ from the specific heat of sapphire for structural relaxation, because of the closeness of the thermal conductivities of iron-based metallic glasses [12] to that of sapphire [8].

Results and discussion

a) Structural relaxation

The thickness of the ribbons decreases as a function of increasing wheel speed, as reported by Greer [1]. In our case, it has been estimated that a difference in thickness of 20 μm would correspond to double the cooling rate in the range from 10^5 to 10^6 deg/s [13].

Following a procedure that has already been described [5, 6], two DSC runs are performed on each sample of $\text{Fe}_{39}\text{Ni}_{36}\text{Cr}_5\text{P}_{14}\text{B}_6$: the first one up to $(T_g + 10)$ K in order to relax the alloy completely, and the second one up to complete crystallization (Fig. 2a). If other scans up to $(T_g + 10)$ K are performed after the first one, no further heat release is observed and the DSC traces overlap, showing that an

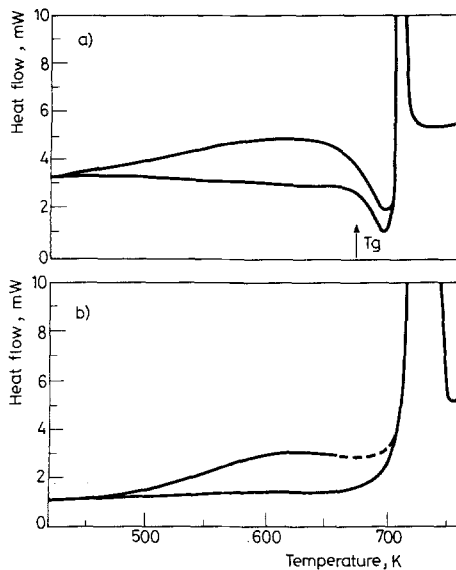


Fig. 2 DSC traces of as-prepared and annealed metallic glasses showing the thermal effect of structural relaxation (see text)

irreversible process has taken place during the first scan. The difference between the apparent specific heat curves (DSC traces) obtained in the two runs are reported in Fig. 3. The area under the curves represents the enthalpy of relaxation. The effect of the quenching rate is clearly seen: the higher the quenching rate, the greater the amount of enthalpy release. Structural relaxation occurs in a wide temperature range and therefore consists of a large number of atomic processes, so that the

whole phenomenon is ruled by a spectrum of activation energies [5, 6]. The broad exothermal peaks show the same features whatever the thickness of the samples; hence, the main effect of the quenching rate is to determine the overall content of frozen-in free volume. The enthalpy of relaxation is alloys $\text{Fe}_{39}\text{Ni}_{36}\text{Cr}_5\text{P}_{14}\text{B}_6$ (0.7, 1.1 and 1.4 kJ/mol for thicknesses of 37, 24 and 16 μm , respectively) is of the same order of magnitude as that found in other metal-metalloid amorphous systems in

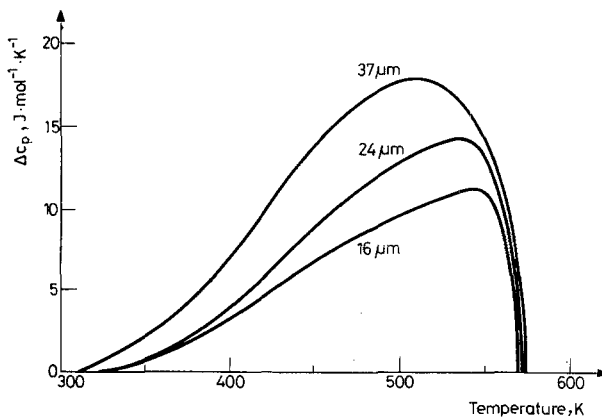


Fig. 3 Difference in apparent specific heat of as-prepared and annealed $\text{Fe}_{39}\text{Ni}_{36}\text{Cr}_5\text{P}_{14}\text{B}_6$ glasses prepared with different quenching rates. Ribbon thickness is reported

ribbon form, such as $\text{Fe}_{75}\text{Si}_{10}\text{B}_{15}$, $\text{Co}_{72.5}\text{Si}_{12.5}\text{B}_{15}$, $\text{Pd}_{48}\text{Ni}_{32}\text{P}_{20}$ [14], $\text{Fe}_{67}\text{Co}_{18}\text{B}_{14}\text{Si}_1$ [15] and $\text{Fe}_{42}\text{Ni}_{41.5}\text{Mo}_5\text{B}_{11.5}$ [5]. It is worth noting that larger differences are found between amorphous alloys of the same composition prepared with different techniques, as in-rotating water spinning, melt spinning and water quenching [14], or melt spinning and sputtering [16], because of the differences in effectiveness of the cooling conditions in each method.

Further, differences in the apparent specific heat curves of the same magnitude were found in some systems showing no manifest T_g : $\text{Fe}_{81}\text{B}_{19}$, $\text{Fe}_{75}\text{V}_4\text{B}_{21}$ and $\text{Fe}_{76}\text{Co}_4\text{B}_{20}$ Fig. 2b). In this case the first DSC run is stopped just before crystallization and, as T_g is never reached, the structural relaxation process never goes to completion. Δc_p curves are shown in Fig. 4. The two curves pertaining to the alloy $\text{Fe}_{75}\text{V}_4\text{B}_{21}$ reveal the effect of the temperature at which heating is interrupted. It is seen that the specific heat difference of the as-quenched sample with respect to the relaxed one is enhanced by an increase of the temperature reached during the first DSC run, so that it is not possible to define a reference state for relaxation in alloys without manifest T_g . Actually, relaxation continues even at higher temperature in a region not accessible to measurement, without producing a partial crystallization (dotted line in Fig. 2b):

The range in which relaxation occurs shifts towards higher temperature values in the $\text{Fe}_{75}\text{V}_4\text{B}_{21}$ system, if compared with $\text{Fe}_{81}\text{B}_{19}$ and $\text{Fe}_{76}\text{Co}_4\text{B}_{20}$. This follows the trend of the crystallization temperature [17] and implies that both phenomena are ruled by the motion of the large vanadium atoms. Substitution of a certain proportion of the Fe atoms by other transition elements leads to an increase in the

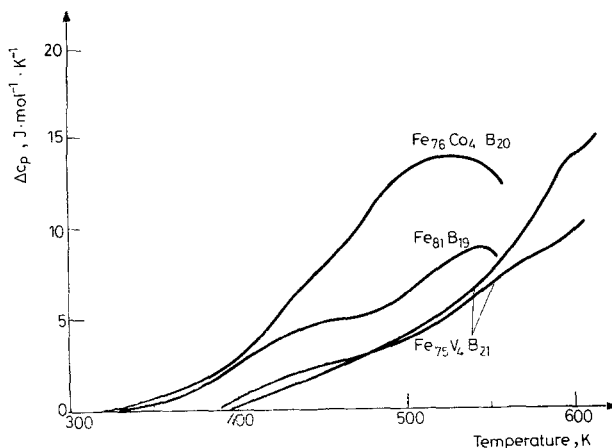


Fig. 4 Difference in apparent specific heat of as-prepared and annealed $\text{Fe}_{81}\text{B}_{19}$, $\text{Fe}_{75}\text{V}_4\text{B}_{21}$, $\text{Fe}_{76}\text{Co}_4\text{B}_{20}$ glassy alloys

apparent Δc_p , which may be associated with a larger quenched-in free volume, but also with a stronger interaction when unlike atoms are put together in an amorphous alloy. Heats referring to the partial relaxation shown in Fig. 4 are 0.6 kJ/mol for $\text{Fe}_{81}\text{B}_{19}$, 0.8 kJ/mol for $\text{Fe}_{75}\text{V}_4\text{B}_{21}$, and 0.9 kJ/mol for $\text{Fe}_{76}\text{Co}_4\text{B}_{20}$, i.e. 10, 18 and 16% of the corresponding heat of crystallization. In fact, for multicomponent alloys such as Fe-Ni-Cr-P-B, the total relaxation reaches more than 50% of the heat of crystallization [5].

b) Heat of crystallization

The specific heats of the alloy before and after crystallization are markedly different, mainly when T_g is manifest (Fig. 2), so that the problem arises of correctly assessing the baseline under the peak. The following iterative procedure was adopted [18]. An approximated baseline is established by drawing a straight line from the onset to the end of the peak, and the total area of the peak is computed. Partial transformed fractions are then computed step by step and a new baseline is obtained by weighing the c_p level on the transformed fractions. A sigmoidal curve is obtained, which is then optimized to convergence by repeating the above procedure

(Fig. 5). Integration is made on a time base, because a strong self-heating effect is observed as a consequence of a very rapid reaction (Fig. 5), even if the experiment is performed with a very small amount of material (about 1 mg).

In the alloys with manifest T_g , $\text{Fe}_{39}\text{Ni}_{36}\text{Cr}_5\text{P}_{14}\text{B}_6$, the heat of crystallization ΔH_x (3.5 ± 0.2 kJ/mol) changes neither as a function of the quenching rate nor in

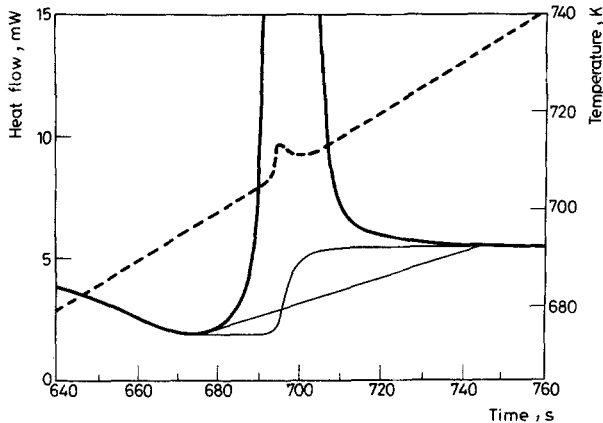


Fig. 5 Baseline construction under a crystallization peak (see text). Dotted line: time-temperature curve showing a self-heating effect

specimens completely relaxed at T_g . Within the accuracy of these data, these results indicate that the structural differences induced by the different cooling rates are completely eliminated when the undercooled liquid state is reached at T_g , so that the specimens behave similarly with respect to crystallization.

More surprisingly, it was found that even in the case of alloys showing no manifest T_g , the heat of crystallization has the same value for as-quenched and relaxed specimens (namely 6.1 ± 0.2 , 5.5 ± 0.2 and 4.5 ± 0.2 kJ/mol for $\text{Fe}_{81}\text{B}_{19}$, $\text{Fe}_{76}\text{Co}_4\text{B}_{20}$ and $\text{Fe}_{75}\text{V}_4\text{B}_{21}$). This shows that the remaining part of the relaxation enthalpy in these cases is negligible with respect to the total heat of crystallization. In the literature, examples of both constant ΔH_x ($\text{Fe}_{71}\text{Si}_{13}\text{B}_{16}$ [19]) and increasing ΔH_x with increasing cooling rate ($\text{Fe}_{40}\text{Ni}_{40}\text{B}_{20}$ [20]) have been reported for metallic glasses without manifest T_g . Even though constancy appears as a more common case, different behaviour can probably be found in alloys giving a high heat of relaxation with partial overlap of crystallization. More experimental data are necessary to clarify this point for a complete understanding of the thermal history of metallic glasses.

References

- 1 A. L. Greer, *J. Mat. Sci.*, 17 (1982) 1117.
- 2 F. E. Luborsky, H. H. Liebermann and J. L. Walter, in Proc. Conf. on Metallic Glasses: Science and Technology, C. Hargitai, I. Bakonyi and T. Kemeny, Kultura, Budapest, 1981, Vol. I, p. 203.
- 3 J. R. Cost and J. T. Stanley, *Scripta Met.*, 15 (1981) 407.
- 4 R. W. Cahn, *Contemp. Phys.*, 21 (1980) 43.
- 5 L. Battezzati, G. Riontino, M. Baricco, A. Lucci and F. Marino, *J. Non-Cryst. Sol.*, 61 & 62 (1984) 877.
- 6 H. S. Chen, *J. Non-Cryst. Sol.*, 46 (1981) 289.
- 7 R. Hultgren, P. D. Desai, D. T. Hawkins, M. Gleiser, K. K. Kelly and D. D. Wagman, Selected Values of Thermodynamic Properties of the Elements, American Society of Metals, Metals Park, Ohio, 1973.
- 8 R. C. Weast, Handbook of Chemistry and Physics, CRC Press, Boca Raton, Florida, 1983.
- 9 D. C. Ginnings and G. T. Furukawa, *J. Am. Chem. Soc.*, 75 (1953) 522.
- 10 W. Eysel and K. H. Breuer, in Thermal Analysis Proc. 7th ICTA, B. Miller, J. Wiley, Chichester, 1982, Vol. I, p. 169.
- 11 S. C. Mraw and D. F. Naas, *J. Chem. Thermodyn.*, 11 (1979) 567.
- 12 S. Kavesh, in Metallic Glasses, J. J. Gilman and H. J. Leamy eds., American Soc. for Metals, Metals Park, Ohio, 1976, p. 36.
- 13 M. Baricco, L. Battezzati, F. Marino and G. Riontino, in Proc. 5th Int. Conf. on Rapidly Quenched Metals, S. Steeb and M. Warlimont eds., North Holland, Oxford, 1985, Vol. I, p. 239.
- 14 A. Inoue, T. Masumoto, M. Hagiwara and H. S. Chen, *Scripta Met.*, 17 (1983) 1205.
- 15 M. Harmelin, Y. Calvayrac, A. Quivy, J. Bigot, P. Burmier and M. Fayard, *J. Non-Cryst. Sol.*, 61 & 62 (1984) 931.
- 16 M. Harmelin, A. Naudon, J. M. Frigerio and J. Rivory, in Proc. 5th Int. Conf. on Rapidly Quenched Metals, S. Steeb and M. Warlimont eds., North Holland, Oxford, 1985, Vol. I, p. 659.
- 17 C. Antonione, G. Riontino and G. Venturello, *Mat. Chem. Phys.*, 12 (1985) 199.
- 18 M. G. Scott and P. Ramachandrarao, *Mat. Sci. Eng.*, 29 (1977) 137.
- 19 F. E. Luborsky, J. Reeve, H. A. Davies and H. H. Liebermann, *IEEE Trans. on Magn.*, MAG-18 (1982) 1385.
- 20 R. Gerling and R. Wagner, *Scripta Met.*, 17 (1983) 1129.

Zusammenfassung — Strukturelle Relaxation und Kristallisation der metallischen Gläser $\text{Fe}_{39}\text{Ni}_{36}\text{Cr}_5\text{P}_{14}\text{B}_6$, $\text{Fe}_{81}\text{B}_{19}$, $\text{Fe}_{76}\text{Co}_4\text{B}_{20}$ und $\text{Fe}_{75}\text{V}_4\text{B}_{21}$ wurden mittels DSC untersucht. Verschiedene Koeffizienten zur Kalibrierung der DSC-Zelle wurden für die zwei Phänomene bestimmt. Die Entalpie der Relaxation steigt mit zunehmender Abkühlungsgeschwindigkeit im Falle von $\text{Fe}_{39}\text{Ni}_{36}\text{Cr}_5\text{P}_{14}\text{B}_6$ und mit zunehmender Zahl der Legierungskomponenten im Falle der Fe-B-Gläser an. In den letztgenannten Systemen ist die Relaxation niemals vor Beginn der Kristallisation beendet. Die Entalpie der Kristallisation ist im Falle von $\text{Fe}_{39}\text{Ni}_{36}\text{Cr}_5\text{P}_{14}\text{B}_6$ unabhängig von der Abkühlungsgeschwindigkeit und ändert sich auch nicht beim Tempern im Relaxationsgebiet vor der Kristallisation.

Резюме — Методом ДСК изучены структурная релаксация и кристаллизация металлических стекол состава $\text{Fe}_{39}\text{Ni}_{36}\text{Cr}_5\text{P}_{14}\text{B}_6$, $\text{Fe}_{81}\text{B}_{19}$, $\text{Fe}_{76}\text{Co}_4\text{B}_{20}$ и $\text{Fe}_{75}\text{V}_4\text{B}_{21}$. Для этих двух процессов определен дифференциальный коэффициент калибровки ДСК ячейки. Энтальпия релаксации в $\text{Fe}_{39}\text{Ni}_{36}\text{Cr}_5\text{P}_{14}\text{B}_6$ увеличивается с увеличением скорости закаливания, а в стеклах на основе Fe—B — с увеличением числа компонентов в сплавах. В этих последних сплавах релаксация никогда не была полной перед началом кристаллизации. Энтальпия кристаллизации сплавов $\text{Fe}_{39}\text{Ni}_{36}\text{Cr}_5\text{P}_{14}\text{B}_6$ не зависит от скорости закаливания и не изменялась при отжиге их в релаксационном поле перед кристаллизацией.